

# Exocytotic release of ATP and activation of P2X receptors in dissociated guinea pig stellate neurons

John D. Tompkins and Rodney L. Parsons

*Am J Physiol Cell Physiol* 291:1062-1071, 2006. First published Jun 7, 2006;  
doi:10.1152/ajpcell.00472.2005

---

## You might find this additional information useful...

---

This article cites 59 articles, 26 of which you can access free at:

<http://ajpcell.physiology.org/cgi/content/full/291/5/C1062#BIBL>

Updated information and services including high-resolution figures, can be found at:

<http://ajpcell.physiology.org/cgi/content/full/291/5/C1062>

Additional material and information about *AJP - Cell Physiology* can be found at:

<http://www.the-aps.org/publications/ajpcell>

---

This information is current as of May 1, 2008 .

## Exocytotic release of ATP and activation of P2X receptors in dissociated guinea pig stellate neurons

John D. Tompkins and Rodney L. Parsons

Department of Anatomy and Neurobiology, University of Vermont, Burlington, Vermont

Submitted 22 September 2005; accepted in final form 31 May 2006

**Tompkins, John D., and Rodney L. Parsons.** Exocytotic release of ATP and activation of P2X receptors in dissociated guinea pig stellate neurons. *Am J Physiol Cell Physiol* 291: C1062–C1071, 2006. First published June 7, 2006; doi:10.1152/ajpcell.00472.2005.—Activation of P2X receptors by a  $\text{Ca}^{2+}$ - and soluble *N*-ethylmaleimide-sensitive factor attachment protein receptor (SNARE) protein-dependent release of ATP was measured using patch-clamp recordings from dissociated guinea pig stellate neurons. Asynchronous transient inward currents (ASTICs) were activated by depolarization or treatment with the  $\text{Ca}^{2+}$  ionophore ionomycin (1.5 and 3  $\mu\text{M}$ ). During superfusion with a HEPES-buffered salt solution containing 2.5 mM  $\text{Ca}^{2+}$ , depolarizing voltage steps (–60 to 0 mV, 500 ms) evoked ASTICs on the decaying phase of a larger, transient inward current. Equimolar substitution of  $\text{Ba}^{2+}$  for  $\text{Ca}^{2+}$  augmented the postdepolarization frequency of ASTICs, while eliminating the larger transient current. Perfusion with an ionomycin-containing solution elicited a sustained activation of ASTICs, allowing quantitative analysis over a range of holding potentials. Under these conditions, increasing extracellular [ $\text{Ca}^{2+}$ ] to 5 mM increased ASTIC frequency, whereas no events were observed following replacement of  $\text{Ca}^{2+}$  with  $\text{Mg}^{2+}$ , demonstrating a  $\text{Ca}^{2+}$  requirement. ASTICs were  $\text{Na}^+$  dependent, inwardly rectifying, and reversed near 0 mV. Treatment with the nonselective purinergic receptor antagonist pyridoxal phosphate-6-azophenyl-2',4'-disulfonic acid (PPADS) (10  $\mu\text{M}$ ) blocked all events under both conditions, whereas the ganglionic nicotinic antagonist hexamethonium (100  $\mu\text{M}$  and 1 mM) had no effect. PPADS also blocked the macroscopic inward current evoked by exogenously applied ATP (300  $\mu\text{M}$ ). The presence of botulinum neurotoxin E (BoNT/E) in the whole-cell recording electrode significantly attenuated the ionomycin-induced ASTIC activity, whereas phorbol ester treatment potentiated this activity. These results suggest that ASTICs are mediated by vesicular release of ATP and activation of P2X receptors.

sympathetic; purinergic; neurotransmission; phorbol ester; botulinum toxin

IN ADDITION to its role as a major source of energy, ATP can serve as a neurotransmitter within the mammalian nervous system (9, 28, 39). Release of ATP from central and peripheral nerve terminals requires  $\text{Ca}^{2+}$  influx (4, 48, 53). Once released, the ATP is susceptible to rapid hydrolysis by extracellular enzymes known as ecto-ATPases. Postsynaptic metabotropic (P2Y) and ionotropic (P2X) receptors have high affinity for ATP and transduce the nucleotide release to an intracellular signal.

The P2X receptors mediate fast synaptic transmission by ATP (17, 40, 47). These ligand-gated ion channels are cation-selective, with almost equal permeability to  $\text{Na}^+$  and  $\text{K}^+$ , and have significant permeability to  $\text{Ca}^{2+}$  (3, 28). The inward

current, resulting from direct activation of the channel by ATP, depolarizes the postsynaptic membrane.  $\text{Ca}^{2+}$  influx through the channel can also activate intracellular signaling cascades with longer lasting effects (16).

ATP appears to be an important signaling molecule within the sympathetic nervous system. In the guinea pig, postganglionic sympathetic fibers innervating intestinal arterioles solely use ATP as a transmitter (18). Sympathetic stimulation of the vas deferens is significantly compromised in mice lacking P2X<sub>1</sub> receptors (38). P2X receptors are also expressed within sympathetic ganglia, where ATP signaling may play a role in ganglionic transmission. In the rat, stimulation of preganglionic fibers of the superior cervical ganglia (SCG) releases ATP within the ganglia (55), where P2X receptors are expressed (14, 29). Guinea pig SCG have also been shown to express P2X receptors (58). In culture, guinea pig coeliac and stellate ganglion neurons can utilize ATP as a neurotransmitter (17, 26). Sympathetic fibers from the stellate ganglia innervate the heart. In coculture with ventricular myocytes, the stellate neurons provide purinergic tone to the cardiac myocytes (26). An aberrant release of ATP from sympathetic nerve fibers at dorsal root ganglia has been suggested to play a role in the sympathetic augmentation of neuropathic pain (59).

Purinergic neurotransmission has been investigated in an array of experimental preparations, after first being described using tissue whole-mount preparations of the sympathetic neuroeffector junction (12). The use of extracellular recording and calcium imaging techniques with these preparations has provided the first descriptions of the quantal-like nature of ATP release from single sympathetic varicosities (5, 6, 10, 31). Recently, cultured chromaffin and PC12 cells have been used to study ATP release (19, 25). A more detailed analysis of the molecules involved in the compartmentalization and release of ATP is needed to more fully understand its role as a neurotransmitter.

During earlier studies designed to examine the role of calcium-induced calcium release in the regulation of action potential generation in guinea pig stellate neurons (35), we frequently observed spontaneous transient inward currents. Here we provide a characterization of these events after establishing conditions under which they could readily be observed. We demonstrate that the asynchronous small transient inward currents (ASTICs) were mediated by an exocytotic release of ATP and autologous activation of P2X receptors. This is the first direct physiological data to demonstrate that ATP release from sympathetic neurons can be inhibited by botulinum neurotoxins and potentiated by phorbol esters. Our results indicate

Address for reprint requests and other correspondence: J. D. Tompkins, Univ. of Vermont, College of Medicine, Dept. of Anatomy and Neurobiology, 89 Beaumont Ave., Given D-408, Burlington, VT 05405 (e-mail: john.tompkins@uvm.edu).

The costs of publication of this article were defrayed in part by the payment of page charges. The article must therefore be hereby marked "advertisement" in accordance with 18 U.S.C. Section 1734 solely to indicate this fact.

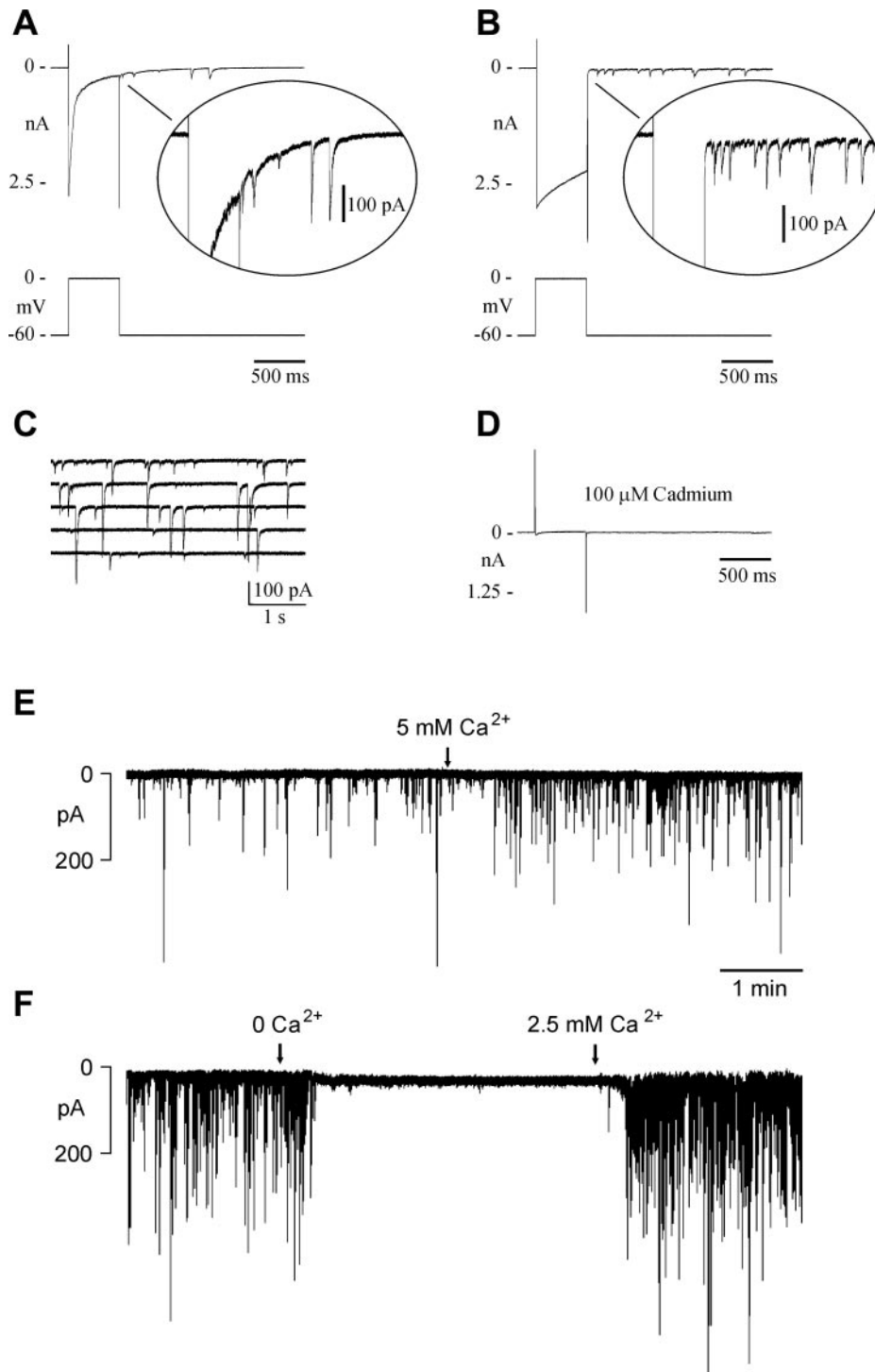


Fig. 1. Asynchronous transient inward currents (ASTICs) can be evoked by depolarizing voltage steps or exposure to the  $\text{Ca}^{2+}$  ionophore ionomycin and require  $\text{Ca}^{2+}$  influx. **A**: under conditions inhibiting voltage-dependent  $\text{Na}^+$  and  $\text{K}^+$  currents, a large transient inward current (top trace) was activated by a depolarizing voltage command (bottom trace). A slowly decaying tail current and multiple ASTICs were observed following repolarization to  $-60$  mV (inset). **B**: equimolar replacement of  $\text{Ba}^{2+}$  for  $\text{Ca}^{2+}$  potentiated the large, voltage-activated inward current, attenuated the tail current, and greatly increased ASTIC frequency. **C**: ASTICs were observed for 25 s following depolarization in  $\text{Ba}^{2+}$  (same cell as **B**). **D**: cadmium inhibited both the voltage-activated inward current and ASTICs. **E**: increasing extracellular  $[\text{Ca}^{2+}]$  from 2.5 to 5 mM, during continuous exposure to the  $\text{Ca}^{2+}$  ionophore ionomycin (1.5  $\mu\text{M}$ ), greatly enhanced the frequency of ASTICs. Cell was held at  $-60$  mV. **F**: substituting  $\text{Mg}^{2+}$  for  $\text{Ca}^{2+}$  during treatment with 3  $\mu\text{M}$  ionomycin reversibly inhibited ASTIC activity.

that these cells may be a useful system to study the regulation of purinergic neurotransmission.

#### MATERIALS AND METHODS

**Ganglion dissection and cell culture.** Stellate ganglia were removed from Hartley guinea pigs (either sex; 250–300 g) using procedures approved by the University of Vermont Institutional Animal Care and Use Committee. These procedures are in accordance with the guidelines established by the National Institutes of Health

*Guide for the Care and Use of Laboratory Animals*. All efforts were made to minimize the number of animals used and their suffering.

Guinea pigs were euthanized by halothane overdose and were exsanguinated. The right and left stellate ganglia were exposed rostral to the first rib, removed, and placed in a bubbled Krebs solution containing (in mM) 120.9 NaCl, 5.9 KCl, 25  $\text{NaHCO}_3$ , 1.2  $\text{NaH}_2\text{PO}_4$ , 2.5  $\text{CaCl}_2$ , 1.2  $\text{MgCl}_2$ , and 11 glucose (bubbled with 95%  $\text{O}_2$ -5%  $\text{CO}_2$ ). The isolated ganglia were pinned to the Sylgard-184 (Dow Corning, Midland, MI) floor of a 35-mm petri dish for removal of the encapsulating connective tissue. The ganglia were minced and enzy-

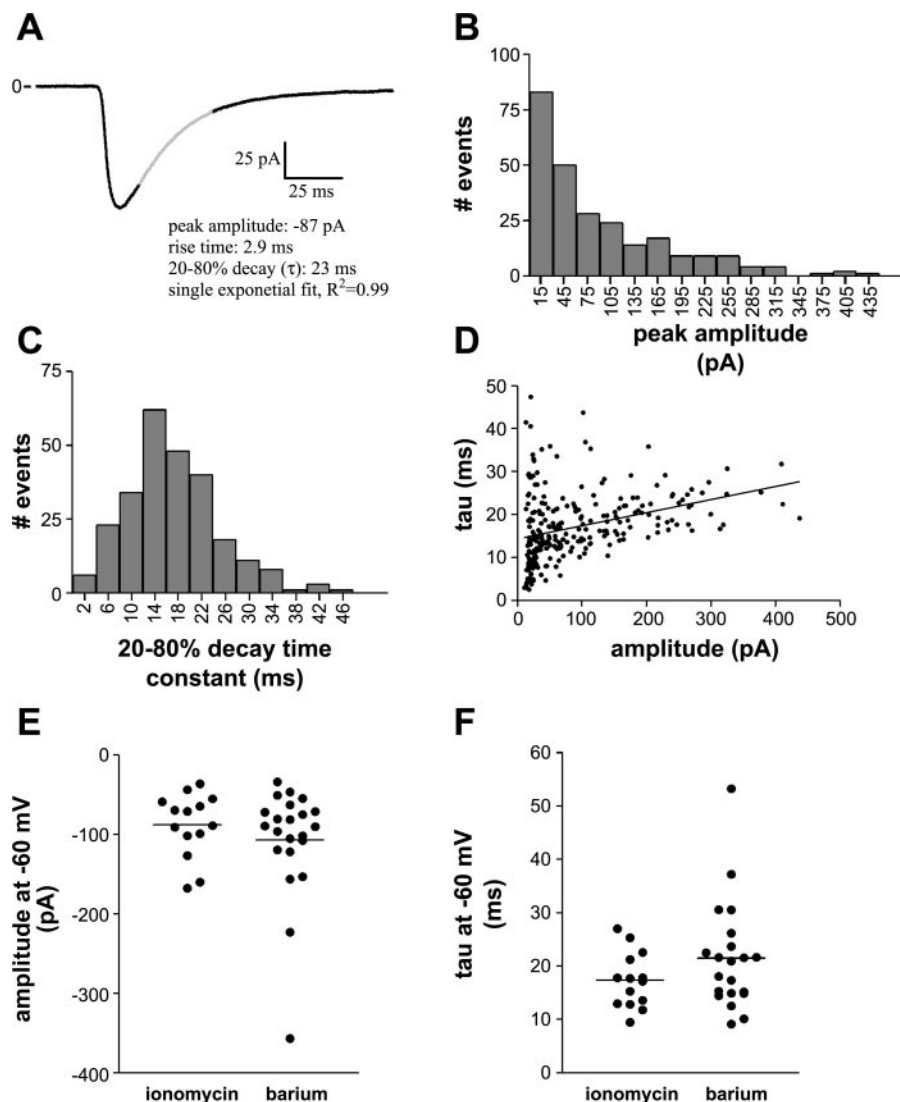


Fig. 2. ASTIC characteristics. *A–D*: results from a single cell treated with ionomycin (3  $\mu$ M) in  $\text{Ca}^{2+}$  (2.5 mM) *A*: average current trace for 260 ASTICs recorded at  $-60$  mV. *B*: frequency histogram showing a skewed distribution of ASTIC amplitudes (shown as absolute value); 30-pA bins, mean =  $-91 \pm 5$  pA, median =  $-56$  pA. *C*: frequency histogram illustrating a normal distribution of the decay time constants ( $\tau$ ) for the same events shown in *B*; 4-ms bins, mean =  $17 \pm 0.5$  ms, median = 16 ms. *D*: linear regression shows no correlation between the two; slope =  $0.03 \pm 0.005$ ,  $r^2 = 0.11$ . *E*: peak event amplitudes were similar under either stimulation condition (ionomycin,  $n = 14$ ; barium,  $n = 22$ ). Each point represents mean value for one cell. Horizontal bars indicate mean of means. *F*: decay time constants were also similar under either treatment protocol.

matically dissociated in 2 ml of a low- $\text{Ca}^{2+}$  HEPES-buffered salt solution containing 121 mM NaCl, 5.9 mM KCl, 26 mM Na-HEPES, 1.2 mM  $\text{MgCl}_2$ , 0.1 mM  $\text{CaCl}_2$ , 8 mM glucose, 3 mg/ml trypsin type XII-S (11,500 BAE units/mg; Sigma-Aldrich, St. Louis, MO), and 10 mg/ml collagenase A (0.25 U/mg; Roche Molecular Biochemicals, Indianapolis, IN). The solution was mixed on a nutator (BD, Franklin Lakes, NJ) in a  $37^\circ\text{C}$  incubator with an atmosphere of 5%  $\text{CO}_2$ -95% air for 1 h. Immediately following the incubation period, the tissue was transferred to 1 ml of “wash” solution for 10 min to quench enzyme activity. The wash solution contained Eagle’s MEM (M7278; Sigma-Aldrich) plus 10% FCS, 0.1% BSA, 0.1 mg/ml pyruvic acid, 1 mg/ml DNase, 200 U/ml penicillin, 0.2 mg/ml streptomycin, and 0.2 mg/ml gentamicin. Tissue was then transferred to 1 ml of the low- $\text{Ca}^{2+}$  HEPES-buffered Krebs and gently triturated to break up the remaining tissue fragments. The solution was serially diluted (1:10) into multiple tubes. Tubes were centrifuged at 100  $g$  for 5 min. The supernatant was discarded, and the remaining pellet was resuspended in a growth medium containing MEM, 2.5 mM  $\text{CaCl}_2$ , 8 mM glucose, 1 mg/ml DNase, 200 U/ml penicillin, 0.2 mg/ml streptomycin, and 0.2 mg/ml gentamicin. Dissociated neurons were seeded on glass coverslips (15 mm; Fisher Scientific, Hampton, NH) and stored in the incubator. The growth medium was replaced after 24 h and supplemented with 10% FCS and 0.1% BSA. Neurons were maintained in

primary culture for 24–48 h and were identified by morphological and electrophysiological characteristics.

**Electrophysiological recordings.** Recordings were made from neurons 24–48 h after dissociation. All experiments were conducted at  $32^\circ\text{C}$  with the temperature maintained by a thermostatically controlled in-line heater (Warner Instruments, Hamden, CT). Whole-cell currents were recorded under voltage-clamp conditions using the perforated patch configuration of the patch-clamp recording technique. Cells were superfused with a HEPES-buffered salt solution (extracellular solution) composed of (in mM) 121 NaCl, 26 Na-HEPES, 5.9 KCl, 1.2  $\text{MgCl}_2$ , and either 2.5  $\text{CaCl}_2$ , or 2.5  $\text{BaCl}_2$  (pH 7.36–7.40). TTX (300 nM) was added to block voltage-dependent  $\text{Na}^+$  channels. Unless otherwise noted, patch pipettes were backfilled with a CsAsp/CsCl recording solution containing 140 mM aspartic acid, 30 mM CsCl, 10 mM HEPES, 5 mM  $\text{MgCl}_2$ , and 0.2 mg/ml amphotericin B (pH 7.15–7.20 with CsOH). Cesium was added to the pipette solution to block voltage-dependent  $\text{K}^+$  currents. Pipette resistances were 3–5  $\text{M}\Omega$  when pipettes were filled with the recording solution, and the electrode shanks were coated with dental wax to reduce electrode capacitance.

To determine whether ASTICs were SNARE protein-dependent, standard whole-cell recordings were made with botulinus type E derivative neurotoxin (BoNT/E) added to the recording solution.

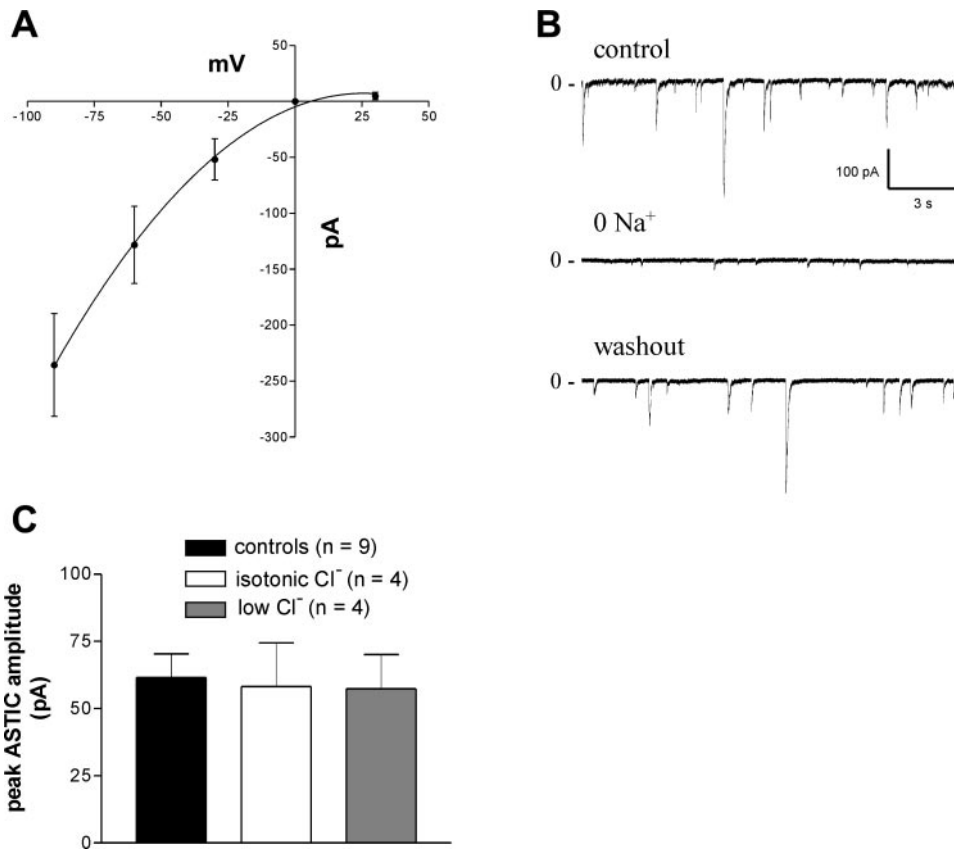


Fig. 3. Ionic nature: ASTICs are Na<sup>+</sup> but not Cl<sup>-</sup> dependent. *A*: current-voltage relationship of mean peak current amplitude. ASTICs were inwardly rectifying and reversed near 0 mV. Each point is the mean  $\pm$  SE for 8 cells. The solid line represents the fit of a second-order polynomial to the data. *B*: ASTIC amplitude was significantly attenuated during perfusion with a Na<sup>+</sup>-free solution (*N*-methyl-D-glucamine<sup>+</sup> substituted for Na<sup>+</sup>). All traces are from a single neuron before, during, and after switching to a Na<sup>+</sup>-free extracellular solution. Traces are representative of responses obtained in 4 cells voltage clamped at a holding potential of  $-60$  mV. In 2 of the 4 cells, no ASTICs were observed after switching to *N*-methyl-D-glucamine<sup>+</sup>. *C*: altering intracellular Cl<sup>-</sup> concentration did not affect mean ASTIC amplitude; control [Cl<sup>-</sup>]<sub>i</sub> = 40 mM, low Cl<sup>-</sup> [Cl<sup>-</sup>]<sub>i</sub> = 10 mM, isotonic Cl<sup>-</sup> [Cl<sup>-</sup>]<sub>i</sub> = 130 mM.

BoNT/E was proteolytically activated by incubating 50  $\mu$ l of BoNT/E (1 mg/ml; Wako Chemicals) with 175  $\mu$ l of bovine pancreatic trypsin (0.3 mg/ml, TPCK treated; Sigma-Aldrich, T1426) in 30 mM HEPES (pH 6.75) at 37°C for 30 min. After incubation, 50  $\mu$ l leupeptin (3 mM; Sigma-Aldrich, L2023) was added to inhibit trypsin. The BoNT/E solution was diluted with 750  $\mu$ l of the whole-cell recording solution containing (in mM) 140 cesium aspartate, 30 CsCl, 5 MgCl<sub>2</sub>, 0.4 NaGTP, 3 MgATP, 3 phosphocreatine, 5 EGTA, and 10 HEPES-CsOH (pH 7.18). Control electrodes contained equivalent amounts of trypsin and leupeptin with no BoNT/E.

Voltage commands were applied and currents were recorded using the Axopatch 200B amplifier coupled with the pCLAMP software (version 8.2) and the Digidata 1322A acquisition board (Axon Instruments, Union City, CA). The analog signal was filtered with a low-pass Bessel filter (2 kHz) and digitized at a sampling rate of 20 kHz for storage on the hard drive of a personal computer. ASTICs were analyzed with the Mini Analysis Program (version 5.6; Synaptosoft, Decatur, GA). Only events with amplitudes  $>2$  times the baseline root-mean-square noise level are included in the analysis. Liquid-junction potentials existed between intracellular and extracellular solutions. The reported membrane potentials have not been corrected for these potentials. When extracellular solutions were changed, the alteration in potential was less than  $-10$  mV (pipette negative; Junction Potential calculator, pCLAMP software suite).

PMA, 4 $\alpha$ -PMA, ionomycin, and pyridoxal phosphate-6-azophenyl-2',4'-disulfonic acid (PPADS) (all purchased from Sigma-Aldrich) were added to the extracellular solution, and were applied by superfusion. ATP, adenosine 5'-( $\alpha,\beta$ -methylene) diphosphate ( $\alpha,\beta$ -meATP), and adenosine 5'-[ $\gamma$ -thio]triphosphate (ATP- $\gamma$ -S) (all at 300  $\mu$ M; Sigma-Aldrich) were applied by local pressure application (Picospritzer; General Valve, Fairfield, NJ) through a  $\sim 5$ - $\mu$ m-diameter "puffer" pipette positioned 50–100  $\mu$ m from the neuron.

*Data analysis.* Data are reported as means  $\pm$  SE. Comparisons between means were made using either a paired or unpaired two-tailed

*t*-test as appropriate. Statistical analysis was done using GraphPad Prism software (version 3.0; San Diego, CA). Differences were considered significant at  $P < 0.05$ .

## RESULTS

*ASTICs evoked in dissociated stellate neurons using two protocols.* Successfully patched cells were held at  $-60$  mV, a value of membrane potential near the reported resting membrane potential of guinea pig sympathetic neurons (13, 24). Membrane currents were activated by 500-ms depolarizing voltage steps from the holding potential to 0 mV. In extracellular solution containing Ca<sup>2+</sup> (2.5 mM), a large, rapidly decaying inward current was recorded concurrent with the depolarizing voltage step (Fig. 1A). ASTICs were observed at the offset of the depolarizing step, superimposed on a large, slowly decaying inward tail current (Fig. 1A, inset). Equimolar replacement of extracellular Ca<sup>2+</sup> with Ba<sup>2+</sup>, a divalent cation with greater permeability through voltage-dependent Ca<sup>2+</sup> channels, increased the amplitude and duration of the depolarization-activated inward current (Fig. 1B). In Ba<sup>2+</sup>, no tail current was recorded; however, subsequent ASTIC activity was greatly enhanced (Fig. 1B, inset) with activity lasting 25 to 130 s (Fig. 1C). ASTICs were observed in 22 of 23 cells tested by depolarizing steps in Ba<sup>2+</sup>. Substitution of Ba<sup>2+</sup> for Ca<sup>2+</sup> did not affect the holding current (data not shown). Addition of 100  $\mu$ M CdCl<sub>2</sub> to either the Ca<sup>2+</sup>- or Ba<sup>2+</sup>-containing solutions blocked the depolarization-activated inward current, the transient tail current observed in Ca<sup>2+</sup>-containing solutions, and ASTICs, suggesting a requirement for Ca<sup>2+</sup> or Ba<sup>2+</sup> influx for all currents (Fig. 1D).

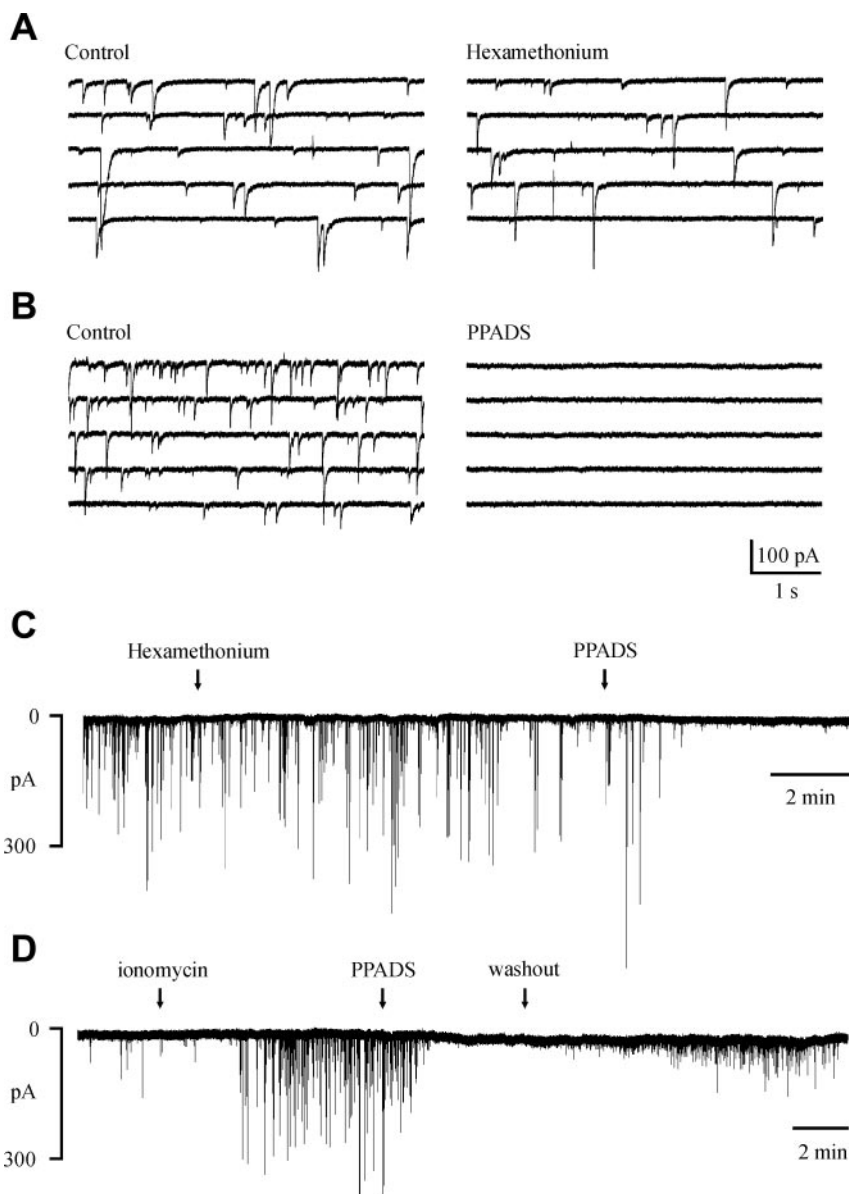


Fig. 4. ASTICs were completely blocked by the purinergic receptor antagonist PPADS. *A*: the ganglionic nicotinic antagonist hexamethonium (100  $\mu$ M) had no effect on ASTICs following a depolarizing voltage step in 2.5 mM  $Ba^{2+}$ . Tracings show 25 s of continuous recording following a depolarizing voltage step before (*left*) and after treatment with hexamethonium (*right*). Cells were superfused with the hexamethonium containing solution for 10 min before repeated depolarization. *B*: ASTICs evoked by depolarization in  $Ba^{2+}$  (*left*) were completely blocked following a 10 min treatment with 10  $\mu$ M pyridoxal phosphate-6-azophenyl-2',4'-disulfonic acid (PPADS) (*right*). The  $Ba^{2+}$  current was unaffected (not shown). *C*: ASTICs induced by ionomycin treatment (1.5  $\mu$ M) were unaffected by hexamethonium (1 mM) but completely blocked by PPADS (10  $\mu$ M). *D*: the inhibition of ASTICs by PPADS was partially reversible. ASTIC amplitudes did not fully recover during the duration of the experiment.

ASTICs could also be evoked without depolarizing steps by exposing cells to the  $Ca^{2+}$  ionophore ionomycin ( $n = 14$ ; Fig. 1E). In  $Ca^{2+}$ -containing extracellular solution, few if any transient inward currents were observed at the holding potential of  $-60$  mV before switching to solution containing either 1.5 or 3  $\mu$ M ionomycin. In ionomycin, ASTIC activity increased gradually following a brief delay ( $\sim 2$  min). Once initiated, the frequency of events reached a steady state after  $\sim 2$  min. ASTIC activity terminated quickly following superfusion with ionomycin-free extracellular solution to wash out the ionophore. Increasing the extracellular concentration of  $Ca^{2+}$  from 2.5 to 5 mM during continuous exposure to ionomycin greatly increased ASTIC frequency ( $n = 4$ ) (Fig. 1E), and superfusion with solution, in which 2.5 mM  $Ca^{2+}$  was replaced by equimolar  $Mg^{2+}$  reversibly inhibited ASTIC activity ( $n = 3$ ) (Fig. 1F). Both observations demonstrated a requirement for  $Ca^{2+}$  influx in ASTIC generation.

ASTICs evoked by  $Ba^{2+}$  depolarization or ionomycin treatment are identical. In  $Ba^{2+}$ , immediately following depolarization, ASTICs occurred at such a high rate that events were superimposed, creating macroscopic currents. As the frequency declined, individual "quantal-like" events were observed. These discrete, quantal-like events were analyzed. Three to four depolarizing steps from  $-60$  to 0 mV were given in  $Ba^{2+}$  to each of 23 cells to evoke an average of  $88 \pm 17$  events per cell. In comparison, ionomycin treatment yielded a steady, high frequency of discrete events. The concentration of ionomycin (1.5 or 3  $\mu$ M) was adjusted to yield the greatest number of events for a single cell. An average of  $187 \pm 35$  events were evoked during a 5- to 10-min treatment with the calcium ionophore during continuous recording at  $-60$  mV ( $n = 14$ ). The analysis of ASTIC amplitudes and decay times for a single cell in ionomycin is shown in Fig. 2, A–D. The mean amplitude of events elicited by depolarization in  $Ba^{2+}$  solution was

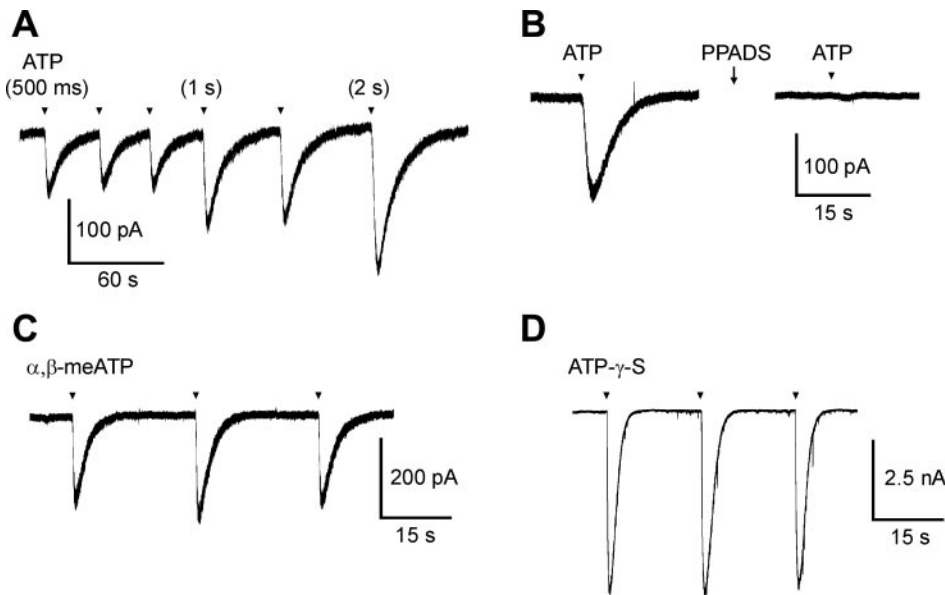


Fig. 5. Dissociated stellate neurons respond to exogenous ATP application. *A*: pressure application of 300  $\mu$ M ATP consistently evoked large transient inward currents. Increasing application duration increased the current amplitude. *B*: PPADS blocked the ATP-evoked response (same cell as *A*). *C*: pressure application of the nonhydrolyzable ATP analog  $\alpha$ ,  $\beta$ -meATP; or *D*: ATP- $\gamma$ -S (both at 300  $\mu$ M) also evoked inward currents.

$-108 \pm 15$  pA, and  $-88 \pm 11$  pA for those evoked by ionomycin in  $\text{Ca}^{2+}$  solution (Fig. 2E). The mean ASTIC amplitudes were not statistically different ( $P = 0.49$ ). The frequency distribution of event amplitudes, determined for cells with  $>60$  events (9 in ionomycin, 19 in  $\text{Ba}^{2+}$ ), was skewed. The example shown in Fig. 2B is for a single cell in ionomycin that is representative of the population distribution observed in all cells. Currents  $<50$  pA occurred with the highest frequency while currents 10-fold greater were also observed.

The falling phase of the inward currents was fit to a single exponential function (Fig. 2A). The decay time constant ( $\tau$ ) of the current was similar for ASTICs evoked in either  $\text{Ba}^{2+}$  or ionomycin. At  $-60$  mV,  $\tau = 22 \pm 2.2$  ms in  $\text{Ba}^{2+}$  and  $17 \pm 1.4$  ms in ionomycin ( $P = 0.26$ , Fig. 2F). The frequency of  $\tau$  was normally distributed (Fig. 2C), and for ASTICs evoked with either stimulation method,  $\tau$  was independent of current amplitude (Fig. 2D).

**ASTIC peak current-voltage relation is inwardly rectifying.** ASTICs exhibited inward rectification at hyperpolarized potentials. The relationship between holding potential and current amplitude is shown in Fig. 3A. To determine the voltage dependence of ASTIC amplitude, cells were clamped at the indicated voltages following depolarizing voltage steps in  $\text{Ba}^{2+}$  or treatment with ionomycin in  $\text{Ca}^{2+}$ . In all cells held at 0 mV, no ASTICs were observed, suggesting that the reversal potential was near zero. Outward currents were only observed in 3 of 10 cells tested at holding potentials  $>0$  mV. These cells showed more robust current intensity overall. In all cells, events recorded at  $-60$  and  $-90$  mV were readily visible and easily analyzed given the low noise and relatively large current amplitude. In contrast, currents recorded at more depolarized potentials were harder to resolve because of the low signal-to-noise ratio. During analysis, if no events exceeded the threshold (see MATERIALS AND METHODS) at a given potential, the current amplitude was recorded as 0 pA. The current amplitudes may therefore be underestimated at positive potentials.

**ASTICs generated by activation of a nonselective cation conductance.** To determine the ionic nature of the transient inward currents, substitutions were made to the recording solutions, and events were evoked by depolarizing steps in  $\text{Ba}^{2+}$ . A reversal potential of  $\sim 0$  mV suggested that ASTICs were generated by activation of a nonselective cation conductance. To test this possibility, *N*-methyl-D-glucamine $^{+}$ , an organic cation, was substituted for  $\text{Na}^{+}$  in the extracellular solution. ASTIC amplitudes were significantly attenuated by superfusion with the  $\text{Na}^{+}$ -free solution (Fig. 3B). In two of four cells tested, no events were detectable at  $-60$  mV following the depolarizing step; thus most of the inward current was eliminated by removal of extracellular  $\text{Na}^{+}$ . However, very small inward currents occasionally remained. Therefore, we tested whether activation of a  $\text{Cl}^{-}$  current might also contribute to ASTIC generation. Shifting the  $\text{Cl}^{-}$  equilibrium potential to a more negative value ( $E_{\text{Cl}^{-}} = -70$  mV), by decreasing the CsCl concentration in the pipette solution, had no effect on ASTIC amplitudes ( $n = 4$ , Fig. 3C). Increasing the  $\text{Cl}^{-}$  concentration to 130 mM in the recording electrode ( $E_{\text{Cl}^{-}} = 0$  mV) also caused no change in ASTIC amplitude ( $n = 4$ , Fig. 3C), although noticeable swelling of the patched neuron was observed while holding the neuron at  $-60$  mV.

**PPADS but not hexamethonium blocked ASTICs.** The rapid onset, small amplitude, and exponential decay of the ASTICs was reminiscent of spontaneous excitatory synaptic currents. To determine whether the evoked currents were receptor mediated, the effect of ligand-gated ion channel antagonists was tested. Treatment with hexamethonium (100  $\mu$ M and 1 mM), a ganglionic nicotinic antagonist, had no effect on the characteristics of ASTICs elicited by either depolarizing voltage steps in  $\text{Ba}^{2+}$  or treatment with ionomycin ( $n = 3$ , Fig. 4, A and C). In contrast, PPADS (10  $\mu$ M), a purinergic antagonist (30, 33), completely inhibited all activity under the same conditions, suggesting all events were P2X receptor mediated (Fig. 4, B–D). During ionomycin treatment, PPADS slowly reduced ASTIC amplitudes until all activity was blocked after  $\sim 2$  min

of treatment. The inhibition by PPADS was partially reversed following washout of PPADS with control solution (Fig. 4D).

To confirm that the dissociated stellate neurons responded to purinergic activation, ATP and two nonhydrolyzable ATP analogs ( $\alpha,\beta$ -meATP and ATP- $\gamma$ -S) were applied to isolated neurons by pressure application (Fig. 5). Puffer pipettes were backfilled with 300  $\mu$ M ATP or an ATP analog, and the drug solutions were applied at close proximity (within 100  $\mu$ m) by pressure ejection onto the patched cells. All agonists evoked large, transient inward currents in each cell tested ( $n = 8$  for ATP, 5 for  $\alpha,\beta$ -meATP, 2 for ATP- $\gamma$ -S). Repetitive application of ATP produced equivalent responses. Increasing the duration of the pressure pulse increased the amplitude of the response. Ten minutes of PPADS (10  $\mu$ M) application completely blocked the ATP response (Fig. 5B).

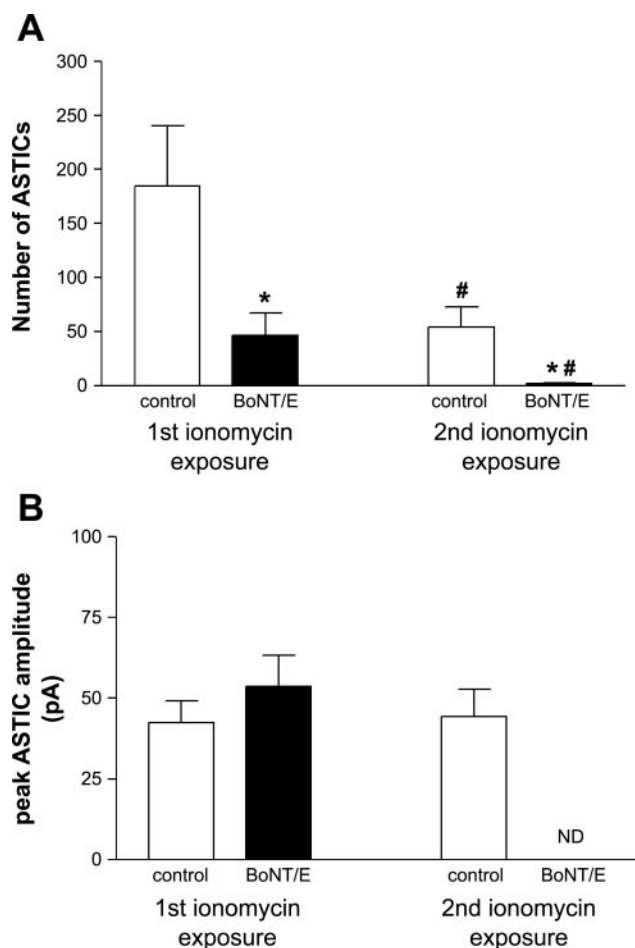


Fig. 6. Inhibition of ASTIC activity following treatment with BoNT/E. *A*: the number of ASTICs evoked during the first 10-min period of ionomycin treatment were significantly reduced by whole-cell electrodes containing botulinum neurotoxin E (BoNT/E). During the second 10-min treatment period, following a 10 min wash, the number of ASTICs was reduced in control cells as well as in BoNT/E-treated cells, although there were significantly fewer events in the BoNT/E-treated cells. Of the BoNT/E treated cells, 2 or fewer events were observed in 5 of the 6 cells during the second ionomycin treatment. *B*: The average ASTIC amplitudes was unaffected by BoNT/E treatment. Event amplitudes were not determined (ND) for BoNT/E treated cells during the second application of ionomycin because too few events were recorded. Recordings were made from a total of 6 cells in both groups. \*significant difference from control (unpaired *t*-test), #significant difference from first ionomycin exposure (paired *t*-test).

*BoNT/E significantly reduced ASTIC activity.* To investigate whether ASTICs were mediated by vesicular release of ATP, cells were directly loaded with BoNT/E via the patch pipette. The protocol for obtaining ASTICs was the same for both control and BoNT/E-treated cells. Patch pipettes were dipped in the standard filling solution and then backfilled with either the BoNT/E solution or the control solution. The membrane patch was ruptured 5 min after obtaining a gigaohm seal, and 10 min of baseline recording was made before switching to an extracellular solution containing ionomycin (1.5  $\mu$ M). The cells were superfused with ionomycin for 10 min, washed with control solution for 10 min, and then treated with ionomycin for a second 10-min period. The total number of ASTICs recorded during each period in ionomycin with both control and BoNT/E electrodes is shown in Fig. 6. The effect of BoNT/E treatment was evidenced by a significant reduction in the number of ASTICs recorded during ionomycin treatment. An average of 185 ± 56 events were recorded with the control electrode solution during the first treatment with ionomycin ( $n = 6$ ) vs. 47 ± 21 events in the BoNT/E-treated cells ( $n = 6$ ,  $P = 0.04$ ). Fewer events were recorded during the second application of ionomycin: 55 ± 18 ( $n = 6$ ) from control and as few as 2 ± 1 ( $n = 6$ ,  $P = 0.02$ ) from the BoNT/E-treated cells.

While the number of events was significantly reduced, ASTIC amplitudes were unaffected by BoNT/E treatment (Fig. 6B). During the first ionomycin treatment period, the peak ASTIC amplitude averaged -43 ± 16 pA in control cells vs. -54 ± 22 pA in the BoNT/E treated-cells ( $P = 0.36$ ). Too few events were recorded from the BoNT/E-treated cells during the second ionomycin exposure period to calculate a mean value. For the control cells, ASTIC amplitudes did not differ between the first (-43 ± 16 pA) and second (-44 ± 19 pA) treatment periods.

*Phorbol esters increase ASTIC activity in ionomycin.* Phorbol esters can enhance synaptic transmission (36). To test whether the phorbol ester PMA could modulate ATP release from the cultured stellate neurons, either PMA or its inactive analog 4 $\alpha$ -PMA was added to the extracellular superfusate (both at 1  $\mu$ M). In the presence of ionomycin (1.5  $\mu$ M), PMA significantly increased ASTIC frequency (Fig. 7C;  $P = 0.003$ ,  $n = 5$ ). A representative experiment is shown in Fig. 7A. Ionomycin was applied alone for ~5 min before application of PMA. The inactive PMA analog, 4 $\alpha$ -PMA, did not have an effect on ASTIC activity (Fig. 7, B and C;  $n = 5$ ). Neither drug affected the mean amplitude of the events (Fig. 7D).

## DISCUSSION

In the present study we demonstrate that the ASTICs observed in dissociated guinea pig stellate neurons are mediated by the regulated release of vesicular ATP and subsequent activation of P2X receptors. Exocytosis of ATP was stimulated by  $Ca^{2+}$  influx either through voltage-dependent calcium channels (VDCCs) or by ionomycin-mediated transport. Release could be inhibited by a botulinum neurotoxin known to interrupt vesicular exocytosis and was facilitated by a phorbol ester known to facilitate neurotransmitter release. The ionic nature of the events and their sensitivity to PPADS indicate activation of P2X receptors.

Characteristic of ATP-gated nonselective cation channels, the inward currents were  $Na^+$  dependent, inwardly rectifying,

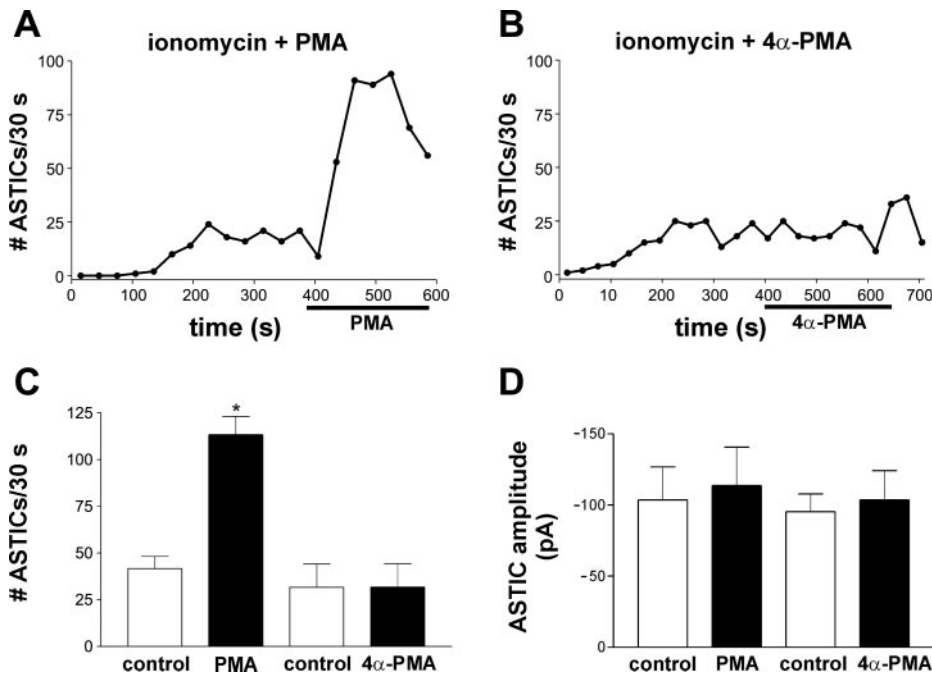


Fig. 7. PMA increases ionomycin-induced frequency of ASTICs. *A* and *B*: frequency histograms illustrate number of ASTICs per unit time (30-s bins) during treatment with ionomycin (1.5  $\mu$ M) and either PMA or 4 $\alpha$ -PMA (both at 1  $\mu$ M). Points indicate bin centers. Ionomycin application began at 0 s and was present throughout the experiment. Duration of application of PMA and 4 $\alpha$ -PMA is illustrated by solid line. Each graph shows results from a representative experiment. *C*: bars show the average number of ASTICs for three points immediately before and after PMA or 4 $\alpha$ -PMA application. \*Significantly different from control ( $P = 0.003$ ;  $n = 5$  for all groups). *D*: the mean amplitude of the events shown in *C* were unaffected by PMA or 4 $\alpha$ -PMA application.

and reversed near 0 mV. This is consistent with previously published observations documenting P2X receptor activation following exogenous application of ATP (29, 34, 46). The noncompetitive P2X receptor antagonist PPADS completely eliminated ASTIC activity following either stimulation protocol. The ganglionic nicotinic antagonist hexamethonium had no effect. The dissociated stellate neurons were also responsive to exogenous application of ATP, which was blocked by PPADS. The nonhydrolyzable ATP analogs,  $\alpha,\beta$ -meATP and ATP- $\gamma$ -S, also effectively evoked responses.

ASTIC kinetics were similar to ATP-mediated excitatory postsynaptic currents (EPSCs) recorded in native tissue. In slice preparations of the medial habenula nucleus, ATP-mediated EPSCs had fast rise times (often  $<2$  ms), and had an exponential decay with a time constant of  $\sim 17$  ms (15). The ASTICs reported here had a rise time of  $\sim 4$  ms, and decayed exponentially with a time constant of  $\sim 17$  ms. In contrast, ATP-mediated currents recorded in cultured clusters of PC12 cells, which lacked synaptic specialization, had slower rise times ( $\sim 9$  ms, measured between 10–90% of the rising time course) and decayed more slowly, with a time constant equal to  $\sim 30$  ms (19). The ASTIC time course is also considerably faster than ATP-mediated transient inward currents recorded from dissociated rat chromaffin cells with heterologously expressed P2X receptors (25).

ASTICs appeared to be mediated by an autocrine signaling pathway with ATP release and P2X receptor activation occurring at the same cell. Events were stimulated and recorded with a single patch electrode from single isolated neurons without visibly attached support cells. Processes were also not evident between cells. Whereas cultured neurons have been demonstrated to form synapses on their own processes or cell bodies, giving rise to “autaptic” connections (2, 21), the presence of a “synaptic-like” connection is not required for neurotransmitter release. Exocytosis may also occur from neuronal cell bodies (42, 54, 57). Additional ultrastructural analysis is needed to

describe the morphological correlates mediating ATP release in the stellate neurons.

ATP has previously been shown to mediate fast excitatory postsynaptic potentials (EPSPs) at P2X receptors with a similar time course to the fast EPSPs evoked by acetylcholine, 5-HT, or glutamate (17, 22). Consistent with its activity as a rapid neurotransmitter, ATP is thought to be contained in synaptic vesicles at nerve terminals, where it is released following action potential-evoked  $\text{Ca}^{2+}$  influx (11, 32, 49, 52). In support of this notion, discrete events correlating with the quantized release of ATP have been recorded from the vas deferens (4, 32).

The characteristics of ASTICs recorded in the stellate neurons are consistent with an exocytotic release mechanism.  $\text{Ca}^{2+}$  influx is a prerequisite for vesicular release of neurotransmitter substances (1). ASTIC activity was  $\text{Ca}^{2+}$  dependent. Blockade of VDCCs with  $\text{Cd}^{2+}$  prevented both the depolarization-induced macroscopic  $\text{Ca}^{2+}$  (or  $\text{Ba}^{2+}$ ) current and activation of the transient inward currents. During ionomycin treatment, ASTIC frequency increased after raising the concentration of extracellular  $\text{Ca}^{2+}$  and was inhibited by omitting external  $\text{Ca}^{2+}$ . The inhibition of ASTICs by BoNT/E also supports the notion of an exocytotic release mechanism. BoNT/E is a zinc metalloendoprotease specific for the synaptosome-associated protein of 25 kDa (SNAP-25) (8). SNAP-25 is an essential constituent of the protein complex (termed the SNARE or core complex) mediating synaptic vesicle exocytosis (44). Treatment of the stellate neurons with BoNT/E resulted in a near complete block of the ionomycin-induced ASTICs after 35 min. The rundown of ASTIC activity observed in the control cells could be attributed to either the washout of intracellular molecules by the whole-cell solution or residual tryptic activity. Despite the observed rundown, the BoNT/E effect was significant. These results are consistent with recently published results demonstrating that botulinum neurotoxin A, which also cleaves SNAP-25, reduces ATP

overflow from sympathetic nerves following field stimulation of isolated canine mesenteric arteries (50).

Neurotransmitter release is a precisely regulated process which can be modulated by intracellular signaling molecules. The second messenger diacylglycerol (DAG) is involved in this regulation. DAG is produced following activation of G protein-coupled receptors. Experiments with phorbol esters, functional analogs to DAG, demonstrate a positive role for these compounds in the regulation of synaptic transmission (37, 45). This effect is attributable to activation of protein kinase C and/or interaction with the synaptic protein munc-13, actions proposed to increase the readily releasable pool and the  $\text{Ca}^{2+}$  sensitivity of the fusion machinery (7, 43, 45, 51, 56). This is the first report that the phorbol ester PMA can enhance the release of ATP from sympathetic neurons. The effect of PMA on ASTIC frequency occurred independently of an effect on ASTIC amplitude. This observation supports the notion that ATP release from the dissociated stellate neurons is a competent release mechanism susceptible to regulation by intracellular factors.

The importance of ATP as a neurotransmitter is demonstrated by its involvement in multiple processes throughout the nervous system including modulation of long-term potentiation, pain transduction, bladder control, modulation of vascular tone, and control of the gastrointestinal system (18, 20, 23, 27, 41). The mechanisms regulating ATP release have been poorly studied. This is due, in part, to the lack of appropriate cellular models that allow for the degree of experimental control necessary to study these mechanisms. Here we demonstrate that ATP release can be readily observed from dissociated sympathetic neurons. This preparation allows for controlled manipulation of the intra- and extracellular environment, making it a good system in future studies to further elucidate mechanisms regulating ATP release.

#### ACKNOWLEDGMENTS

We thank Laura A. Merriam for critical review of an earlier version of the manuscript.

#### GRANTS

This work was supported in part by National Heart, Lung, and Blood Institute (NHLBI) Grant HL-65481. J. D. Tompkins is supported by NHLBI Training Grant HL-07594.

#### REFERENCES

1. **Augustine GJ.** How does calcium trigger neurotransmitter release? *Curr Opin Neurobiol* 11: 320–326, 2001.
2. **Bekkers JM and Stevens CF.** Excitatory and inhibitory autaptic currents in isolated hippocampal neurons maintained in cell culture. *Proc Natl Acad Sci USA* 88: 7834–7838, 1991.
3. **Benham CD and Tsien RW.** A novel receptor-operated  $\text{Ca}^{2+}$ -permeable channel activated by ATP in smooth muscle. *Nature* 328: 275–278, 1987.
4. **Bennett MR.** Autonomic neuromuscular transmission at a varicosity. *Prog Neurobiol* 50: 505–532, 1996.
5. **Bennett MR and Barden JA.** Ionotropic (P2X) receptor dynamics at single autonomic varicosities. *Neuroreport* 12: A91–97, 2001.
6. **Bennett MR, Robinson J, Phipps MC, Karunanithi S, Lin YQ, and Cottee L.** Quantal components of spontaneous excitatory junction potentials at visualized varicosities. *J Auton Nerv Syst* 56: 161–174, 1996.
7. **Betz A, Ashery U, Rickmann M, Augustin I, Neher E, Südhof TC, Rettig J, and Brose N.** Munc13–1 is a presynaptic phorbol ester receptor that enhances neurotransmitter release. *Neuron* 21: 123–136, 1998.
8. **Binz T, Blasi J, Yamasaki S, Baumeister A, Link E, Südhof TC, Jahn R, and Niemann H.** Proteolysis of SNAP-25 by types E and A botulinum neurotoxins. *J Biol Chem* 269: 1617–1620, 1994.
9. **Boehm S.** Signaling via nucleotide receptors in the sympathetic nervous system. *Drug News Perspect* 16: 141–148, 2003.
10. **Brain KL, Jackson VM, Trout SJ, and Cunnane TC.** Intermittent ATP release from nerve terminals elicits focal smooth muscle  $\text{Ca}^{2+}$  transients in mouse vas deferens. *J Physiol* 541: 849–862, 2002.
11. **Brock JA and Cunnane TC.** Relationship between the nerve action potential and transmitter release from sympathetic postganglionic nerve terminals. *Nature* 326: 605–607, 1987.
12. **Burnstock G.** Purinergic nerves. *Pharmacol Rev* 24: 509–581, 1972.
13. **Cassell JF, Clark AL, and McLachlan EM.** Characteristics of phasic and tonic sympathetic ganglion cells of the guinea-pig. *J Physiol* 372: 457–483, 1986.
14. **Connolly GP.** Evidence from desensitization studies for distinct receptors for ATP and UTP on the rat superior cervical ganglion. *Br J Pharmacol* 112: 357–359, 1994.
15. **Edwards FA, Gibb AJ, and Colquhoun D.** ATP receptor-mediated synaptic currents in the central nervous system. *Nature* 359: 144–147, 1992.
16. **Egan TM and Khakh BS.** Contribution of calcium ions to P2X channel responses. *J Neurosci* 24: 3413–3420, 2004.
17. **Evans RJ, Derkach V, and Surprenant A.** ATP mediates fast synaptic transmission in mammalian neurons. *Nature* 357: 503–505, 1992.
18. **Evans RJ and Surprenant A.** Vasoconstriction of guinea-pig submucosal arterioles following sympathetic nerve stimulation is mediated by the release of ATP. *Br J Pharmacol* 106: 242–249, 1992.
19. **Fabbro A, Skorinkin A, Grandolfo M, Nistri A, and Giniatullin R.** Quantal release of ATP from clusters of PC12 cells. *J Physiol* 560: 505–517, 2004.
20. **Ford AP, Gever JR, Nunn PA, Zhong Y, Cefalu JS, Dillon MP, and Cockayne DA.** Purinoceptors as therapeutic targets for lower urinary tract dysfunction. *Br J Pharmacol* 147, Suppl 2: S132–S143, 2006.
21. **Furshpan EJ, MacLeish PR, O'Laigue PH, and Potter DD.** Chemical transmission between rat sympathetic neurons and cardiac myocytes developing in microcultures: evidence for cholinergic, adrenergic, and dual-function neurons. *Proc Natl Acad Sci USA* 73: 4225–4229, 1976.
22. **Galligan JJ and Bertrand PP.** ATP mediates fast synaptic potentials in enteric neurons. *J Neurosci* 14: 7563–7571, 1994.
23. **Galligan JJ and North RA.** Pharmacology and function of nicotinic acetylcholine and P2X receptors in the enteric nervous system. *Neurogastroenterol Motil* 16, Suppl 1: 64–70, 2004.
24. **Gilbert R, Ryan JS, Horackova M, Smith FM, and Kelly ME.** Actions of substance P on membrane potential and ionic currents in guinea pig stellate ganglion neurons. *Am J Physiol Cell Physiol* 274: C892–C903, 1998.
25. **Hollins B and Ikeda SR.** Heterologous expression of a P2x-purinoceptor in rat chromaffin cells detects vesicular ATP release. *J Neurophysiol* 78: 3069–3076, 1997.
26. **Horackova M, Huang MH, and Armour JA.** Purinergic modulation of adult guinea pig cardiomyocytes in long term cultures and co-cultures with extracardiac or intrinsic cardiac neurones. *Cardiovasc Res* 28: 673–679, 1994.
27. **Jo YH and Schlichter R.** Synaptic corelease of ATP and GABA in cultured spinal neurons. *Nat Neurosci* 2: 241–245, 1999.
28. **Khakh BS.** Molecular physiology of P2X receptors and ATP signalling at synapses. *Nat Rev Neurosci* 2: 165–174, 2001.
29. **Khakh BS, Humphrey PP, and Surprenant A.** Electrophysiological properties of P2X-purinoceptors in rat superior cervical, nodose and guinea-pig coeliac neurones. *J Physiol* 484: 385–395, 1995.
30. **Lambrecht G.** Agonists and antagonists acting at P2X receptors: selectivity profiles and functional implications. *Naunyn Schmiedeberg's Arch Pharmacol* 362: 340–350, 2000.
31. **Lamont C and Wier WG.** Evoked and spontaneous purinergic junctional  $\text{Ca}^{2+}$  transients (jCaTs) in rat small arteries. *Circ Res* 91: 454–456, 2002.
32. **Lavidis NA and Bennett MR.** Probabilistic secretion of quanta from visualized sympathetic nerve varicosities in mouse vas deferens. *J Physiol* 454: 9–26, 1992.
33. **Li C.** Novel mechanism of inhibition by the P2 receptor antagonist PPADS of ATP-activated current in dorsal root ganglion neurons. *J Neurophysiol* 83: 2533–2541, 2000.
34. **Liu DM and Adams DJ.** Ionic selectivity of native ATP-activated (P2X) receptor channels in dissociated neurones from rat parasympathetic ganglia. *J Physiol* 534: 423–435, 2001.

35. **Locknar SA, Barstow KL, Tompkins JD, Merriam LA, and Parsons RL.** Calcium-induced calcium release regulates action potential generation in guinea-pig sympathetic neurones. *J Physiol* 555: 627–635, 2004.
36. **Majewski H and Iannazzo L.** Protein kinase C: a physiological mediator of enhanced transmitter output. *Prog Neurobiol* 55: 463–475, 1998.
37. **Malenka RC, Madison DV, and Nicoll RA.** Potentiation of synaptic transmission in the hippocampus by phorbol esters. *Nature* 321: 175–177, 1986.
38. **Mulryan K, Gitterman DP, Lewis CJ, Vial C, Leckie BJ, Cobb AL, Brown JE, Conley EC, Buell G, Pritchard CA, and Evans RJ.** Reduced vas deferens contraction and male infertility in mice lacking P2X1 receptors. *Nature* 403: 86–89, 2000.
39. **Nörenberg W and Illes P.** Neuronal P2X receptors: localisation and functional properties. *Naunyn Schmiedebergs Arch Pharmacol* 362: 324–339, 2000.
40. **North RA.** Molecular physiology of P2X receptors. *Physiol Rev* 82: 1013–1067, 2002.
41. **Pankratov YV, Lalo UV, and Krishtal OA.** Role for P2X receptors in long-term potentiation. *J Neurosci* 22: 8363–8369, 2002.
42. **Puopolo M, Hochstetler SE, Gustincich S, Wightman RM, and Raviola E.** Extrasynaptic release of dopamine in a retinal neuron: activity dependence and transmitter modulation. *Neuron* 30: 211–225, 2001.
43. **Rhee JS, Betz A, Pyott S, Reim K, Varoqueaux F, Augustin I, Hesse D, Südhof TC, Takahashi M, Rosenmund C, and Brose N.** Beta phorbol ester- and diacylglycerol-induced augmentation of transmitter release is mediated by Munc13s and not by PKCs. *Cell* 108: 121–133, 2002.
44. **Rizo J and Südhof TC.** Snares and Munc18 in synaptic vesicle fusion. *Nat Rev Neurosci* 3: 641–653, 2002.
45. **Shapira R, Silberberg SD, Ginsburg S, and Rahamimoff R.** Activation of protein kinase C augments evoked transmitter release. *Nature* 325: 58–60, 1987.
46. **Silinsky EM and Gerzanich V.** On the excitatory effects of ATP and its role as a neurotransmitter in coeliac neurons of the guinea-pig. *J Physiol* 464: 197–212, 1993.
47. **Silinsky EM, Gerzanich V, and Vanner SM.** ATP mediates excitatory synaptic transmission in mammalian neurones. *Br J Pharmacol* 106: 762–763, 1992.
48. **Silinsky EM, Hirsh JK, Searl TJ, Redman RS, and Watanabe M.** Quantal ATP release from motor nerve endings and its role in neurally mediated depression. *Prog Brain Res* 120: 145–158, 1999.
49. **Silinsky EM and Redman RS.** Synchronous release of ATP and neurotransmitter within milliseconds of a motor nerve impulse in the frog. *J Physiol* 492: 815–822, 1996.
50. **Smyth LM, Breen LT, and Mutafova-Yambolieva VN.** Nicotinamide adenine dinucleotide is released from sympathetic nerve terminals via a botulinum neurotoxin A-mediated mechanism in canine mesenteric artery. *Am J Physiol Heart Circ Physiol* 290: H1818–H1825, 2006.
51. **Stevens CF and Sullivan JM.** Regulation of the readily releasable vesicle pool by protein kinase C. *Neuron* 21: 885–893, 1998.
52. **Stjärne L.** Do sympathetic nerves release noradrenaline in “quanta”? *J Auton Nerv Syst* 81: 236–243, 2000.
53. **Stjärne L and Stjärne E.** Geometry, kinetics and plasticity of release and clearance of ATP and noradrenaline as sympathetic cotransmitters: roles for the neurogenic contraction. *Prog Neurobiol* 47: 45–94, 1995.
54. **Trueta C, Mendez B, and De-Miguel FF.** Somatic exocytosis of serotonin mediated by L-type calcium channels in cultured leech neurones. *J Physiol* 547: 405–416, 2003.
55. **Vizi ES, Liang SD, Sperlagh B, Kittel A, and Juranyi Z.** Studies on the release and extracellular metabolism of endogenous ATP in rat superior cervical ganglion: support for neurotransmitter role of ATP. *Neuroscience* 79: 893–903, 1997.
56. **Waters J and Smith SJ.** Phorbol esters potentiate evoked and spontaneous release by different presynaptic mechanisms. *J Neurosci* 20: 7863–7870, 2000.
57. **Zaidi ZF and Matthews MR.** Exocytotic release from neuronal cell bodies, dendrites and nerve terminals in sympathetic ganglia of the rat, and its differential regulation. *Neuroscience* 80: 861–891, 1997.
58. **Zhong Y, Dunn PM, and Burnstock G.** Guinea-pig sympathetic neurons express varying proportions of two distinct P2X receptors. *J Physiol* 523: 391–402, 2000.
59. **Zhou J, Chung K, and Chung JM.** Development of purinergic sensitivity in sensory neurons after peripheral nerve injury in the rat. *Brain Res* 915: 161–169, 2001.